Theoretical modeling of the mechanism of dioxygen activation and evolution by tetranuclear manganese complexes

Davide M. Proserpio*
Istituto di Chimica Strutturistica Inorganica, Universita di Milano, via Venezian 21, 20133 Milan (Italy)

Anthony K. Rappé
Department of Chemistry, Colorado State University, Fort Collins, CO 80523 (USA)

Sergiu M. Gorun*
Exxon Research and Engineering Company, Corporate Research Laboratories, Annandale, NJ 08801 (USA)

(Received June 22, 1993)

Abstract

Oxygen evolution mechanisms at polynuclear manganese centers of the type present in Photosystem II (PSII) are studied using a combination of molecular mechanics and extended Hückel (EH) computational techniques. The energies of two complexes containing peroxo groups bound at a dinuclear ('dimer') subset of tetranuclear ('dimer-of-dimers') Mn aggregates are minimized using the universal force field (UFF) technique. The resulting geometric parameters are in reasonable agreement with those of known Mn peroxo structures. The total energy variation resulting from the structural distortions that accompany the change of the O–O bond order from 0.01 (no bond) to 1.0 indicates lower 'oxygen activation' barriers compared with previous models. Mn bound Cl is found to reduce the net charge on the metal to which it is attached. The equilibrium geometries of the peroxo bound tetranuclear models reveal asymmetric coordination of the peroxo oxygen (Mn–O–O–Mn torsion angles of approx. 60°) consistent with ground state (triplet) oxygen release by PSII. Removal of the two Mn ions which are not directly bound to the peroxide ligand is found to disfavor the oxygen–oxygen coupling by 0.3 eV. Based on the above results a water oxidation mechanism is proposed.

Introduction

Catalytic oxidation chemistry using oxygen as an oxidant is an area of intense research [1–8]. One of the most important problems that remains to be solved is the elucidation of the mechanism of dioxygen activation. In biological systems this activation usually takes place at the metal centers of metalloenzymes. Oxidation catalysts used in industry also contain metals at their active sites. The majority of oxygen-activating enzymes reduce O_2 by two or four electrons to peroxide, O_2^{2-}, or oxide, $2O^{2-}$, respectively. The reverse process, the four electron oxidation of two oxide ions (from two water molecules) to O_2 is performed by the water oxidizing catalyst (WOC) of the photosynthetic apparatus (Photosystem II, PSII) of green plants, algae and cyanobacteria.

The structure of the WOC is currently under direct investigation by a number of groups [9–22]. A likely spectroscopic model [9] of the Mn_4 active site of WOC is presented in Fig. 1. The geometry of this model is derived primarily from X-ray absorption studies [9, 15, 17]. Each of the four manganese centers are octahedrally coordinated, mainly by oxygens. Chloride ions, which are required for activity [16], may also be bound to the Mn center. Current EXAFS results are inconsistent

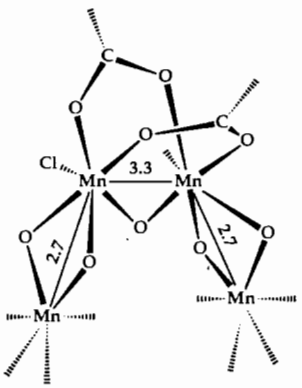

Fig. 1. Proposed spectroscopic model for the manganese center of Photosystem II. Mn–Mn distances are given in angstroms. Adapted from ref. 9.

*Authors to whom correspondence should be addressed.

0020-1693/93/$6.00

with the presence of either two (or more) terminal or one bridging chloride at the metal center. A single, terminal chloride, however, cannot be ruled out [9]. The position of this chloride (if any) may be *cis* to a bridging carboxylate group.

In order to accumulate the four oxidizing equivalents needed for the removal of four electrons from two water molecules, the Mn aggregate of WOC passes through five distinct oxidation states, S_0 to S_4 [23]. The most oxidized one, S_4, which is responsible for O_2 evolution, is believed to contain mainly Mn(IV) [24].

Oxygen evolving experiments using ^{18}O labeled H_2O_2 suggest that during photochemical water oxidation the crucial O–O bond formation step occurs in the S_3 or S_4 state [25]. Interestingly, in the absence of light, the WOC catalyzes the decomposition of hydrogen peroxide into water and oxygen (catalatic activity) [26]. This two-electron redox process is believed to involve only the S_0 and S_2 states. Importantly, manganese bound peroxo groups are produced during both photochemical water oxidation and H_2O_2 decomposition.

Direct investigations have been complemented by numerous modeling studies which have greatly advanced our understanding of the spectroscopic properties and topology of the WOC [13, 27–33]. A previous report presented the synthesis and characterization of an S_0 state model that displays biomimetic catalatic activity [29]. This model, designated model **0**, is shown schematically in Fig. 2. The metal topology and the short O–O distance found in the μ_4-(O–H–O) group prompted the introduction of speculative O_2 evolution mechanisms based, *inter alia*, upon theoretical extended Hückel (EH) calculations [34]. The minimum energy pathway for O–O bond formation was found to be the coupling of the two μ_2 oxygens to form a μ_4-(O–O) group. One of the major difficulties of this approach, however, was the lack of a minimum energy conformation for the peroxo bridged Mn_4 complex, the model for the S_4 state.

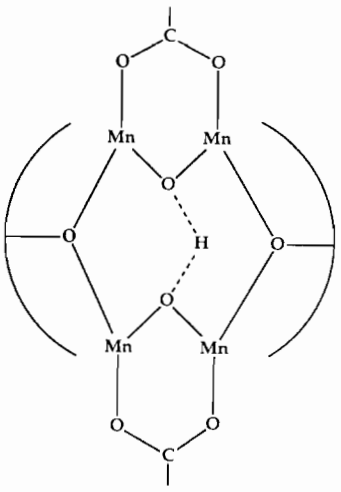

Fig. 2. Schematic representation of model **0**. Only the oxygens of alkoxide and carboxylate groups are shown explicitly.

The work described in this paper is aimed at theoretically modeling the oxygen evolving S_4 state using a combination of molecular mechanics and extended Hückel computational techniques. Our major goals are to understand the structural constraints of polynuclear manganese aggregates that lead to 'oxygen activation' and to introduce a new computational methodology that combines structural minimization via molecular mechanics with one-electron molecular orbital calculations.

The tetranuclear manganese models

Based upon model **0** and the spectroscopic model of Fig. 1 we propose two related topologies for the S_4 state (see Fig. 3), models **1** and **2**. These complexes include four Mn ions octahedrally coordinated by oxygen donors, as suggested by the spectroscopic model. A 'dimer of dimers' topology present in both the WOC model and model **0** is preserved. Formate groups that

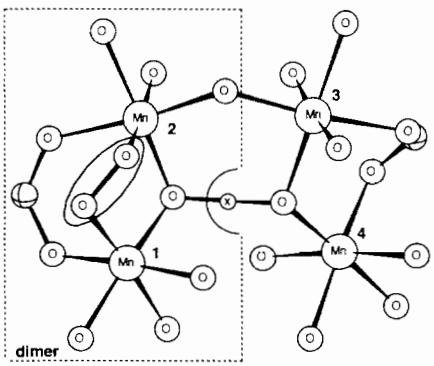

1

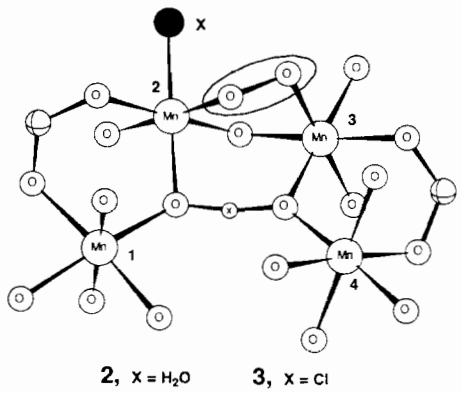

2, X = H_2O **3**, X = Cl

Fig. 3. Schematic representation of models **1**, **2** and **3** and the peroxo-bridged 'dimer' of model **1**. Hydrogens, with the exception of that of the μ_4,η^2-(O–H–O) unit (labeled x) are omitted for the sake of clarity.

approximate carboxylate residues bridge the two Mn centers within each 'dimer'. Bridging oxo and O–H–O groups (the latter observed in model **0**) link the two 'dimers'. Terminal water molecules complete the octahedral coordination sites of the Mn centers. The peroxo group bridges only two metal ions, in an 'intra' dimer (model **1**) or 'inter' dimer (model **2**) fashion, respectively. Due to the trapezoidal metal framework the peroxo groups cannot bridge all four manganese centers. A third model, model **3**, was obtained by substituting an aqua ligand *cis* to the carboxylate group by a terminal chloride (see Fig. 1 for a similar conformation). In order to compare di- and tetranuclear models a peroxo bridged 'dimer' obtained by 'cutting' model **1** (see Fig. 3) was also calculated.

Computational methodology

The geometries of tetranuclear manganese complexes were calculated with the recently introduced molecular mechanics force field, the universal force field (UFF) [35–37]. The viability of this method was initially tested on model **0** which has been structurally characterized. The minimized structure was in reasonable agreement with the X-ray results [29]. In order to take into account the presence of Mn(III) and Mn(IV) in models **1** and **2**, a higher oxidation state Mn center was added to the force field by shrinking the UFF Mn(II) radius by 0.05 Å. The water molecules were attached to the metal centers with bond order 0.5 (due to the dative nature of the bonding). The metal to oxygen formate bonds were assigned bond orders of 0.75, which is the average of 0.5 (dative bond order) and 1 (polar covalent bond order). The formate C–O bonds were each assigned bond order 1.5, the average of a single and a double bond. The initial trial structures (O–O peroxo bond order of 1) were each subjected to two passes of 20 cycles of an annealed dynamics protocol. Each resulting low energy structure was subjected to a charge equilibration-minimization optimization sequence until the energy converged to below 0.1 kcal/mol and the norm of the gradient was less than 0.01 kcal/mol/Å. The lowest energy structure from the first pass of annealed dynamics was used as the starting guess for the second pass. Starting with the lowest energy structures of these models the peroxo O–O bond order was varied as follows: 1.0; 0.75; 0.5; 0.25; 0.1; 0.01. The lower bond order structures were minimized, but not subjected to annealed dynamics. The coordinates of the minimized structures were used in the EH calculations following the strategy described previously [34]*. Although this method is not accurate in calculating absolute energy values, it can model well general orbital energies and major charge shifts. It is within the spirit of the EH method to assume the same parameters for all oxidation states of a transition metal and look for differences due only to variable electron occupancy. It should be noted, however, that the metal–ligand bond distances vary with the metal oxidation state because the radii used in the UFF minimizations are oxidation state dependent.

*The computations were done using the extended Hückel method [38, 39], with weighted H_{ij}s [40], as implemented in a computer program named CACAO, described elsewhere [41]. The parameters used in the calculations are reported in ref. 34.

Results and discussion

Tetranuclear models

Selected geometric parameters for the minimized models are compared in Table 1 with the geometries of X-ray characterized μ,η^2-peroxo manganese complexes. The Mn–O oxo and peroxo distances are similar to those observed for complex **A** which contains Mn(IV). The peroxo bonds, 1.3 Å, are somewhat shorter than the observed 1.46(3) Å because the UFF oxygen radius was obtained from C–O linkages rather than the longer O–O peroxide bonds. The Mn–O–O–Mn torsion angles, ~58°, are substantially larger than the ~0° angles observed for complexes **A** and **B**. The significance of this difference will be discussed later (see below). The Mn–Mn distances are also in reasonable agreement with those observed for complexes **A** and **B**. Interestingly, for both models **1** and **2**, the binding of a peroxide ion at a dinuclear Mn center results in Mn–Mn distances of 2.9–3.0 Å, slightly longer than the 2.7 Å distances observed for the WOC spectroscopic model. The distances between the Mn centers which are not bridged by peroxide, 3.2–3.3 Å, are also consistent with the 3.7 Å distance observed for the WOC (see Fig. 1).

The use of UFF allowed us to compute a possible structural distortion that accompanies the formation of O_2 at a Mn_4 center by varying the bond order (BO) of the O–O bond form 0.01 to 1.0. The starting geometries (BO = 0.01) differ from the final ones (BO = 1.0) mainly in the O–O distances which vary from 2.0 to 1.3 Å. Some rearrangement of the adjacent Mn ions is also observed. Computation of the total energy for oxygen–oxygen bond formation assumed the initial oxidation state of Mn to be formally four. The Walsh diagrams obtained for the present UFF models are formally equivalent with the one reported and analyzed in detail previously [34]. In order to simulate the formation of a peroxo group from two O^{2-}, the electrons are redistributed between O^{2-} and Mn orbitals in the following way. We start with $Mn(IV)_4$, populating the twelve levels of the 't_{2g}' sets with twelve unpaired electrons, thus modeling a high spin $Mn(IV)_4$ ($S = 6$) set. This corresponds to a hypothetical state, the so-

TABLE 1. Selected geometric parameters for peroxo bridged manganese complexes

	Model **1**	Model **2**	Complex **A**[a]	Complex **B**[b]
Mn oxidation states	IV	IV	IV	III
Bridging groups	O_2, OHO, HCOO	O_2, OHO, O	O_2, $(O)_2$	O_2, (O-Mn)
Mn–Mn (Å)	2.93[c]	2.98[d]	2.531(7)	3.14(4)
Mn–O peroxo (Å)	1.86	1.87	1.83(2)	2.0(1)
Mn–O oxo (Å)		1.84	1.81(2)	1.9(1)
O–O peroxo (Å)	1.31	1.32	1.46(3)	1.6(1)
Mn–O–O–Mn torsion angle (°)	59	56	3.1[e]	0.0

[a]$[L_2Mn_2(O)_2(O_2)](ClO_4)_2$, L = 1,4,7-triazacyclononane [42]. [b]$Mn_3L_3(OAc)_2I_3O_3H_2O$, L = diethylenetriamine [43]. [c]3.41 and 3.21 Å in the absence of the bridging peroxo group. [d]3.21 and 3.25 Å in the absence of the bridging peroxo group. [e]Calculated using the atomic coordinates given in ref. 42.

called 'nascent' S_4 state, having the same number of electrons as the S_4 state, yet possessing the assumed structure of the S_3 state which does not contain a peroxide ion. Moving along the reaction coordinate, the highest possible multiplicity is kept (without occupying the antibonding Mn–O 'e_g' set). Transferring electrons from O^{2-} to Mn(IV) results in the formation of a peroxo bridge and of an Mn_2(III)Mn_2(IV) complex with intermediate spin state $S = 5$. The resulting S_4 oxidation state is a precursor to the 'nascent' S_4 state.

Table 2 lists the total energy variation (ΔE) for oxygen coupling and the net charges on Mn and O for the different models. The two electrons transferred from the oxygens distribute unevenly over the four manganese: there is charge buildup on the manganese centers which are *not* directly bonded to dioxygen (not underlined in the Table). The differences in total energies (ΔE) result principally from changes in the energies of the MOs involved in the oxygen–oxygen bond. Comparison of ΔE for these models with those calculated previously starting with model **0** (see above) [34] shows that models **1** and **2** have lower 'oxygen activation' barriers.

The introduction of a chloride ligand does not seem to affect the overall process; it merely reduces the net charges on the Mn directly bonded to it. The geometry of the peroxo group deserves some comment. As has already been pointed out, an asymmetric, twisted coordination of the O–O unit (i.e. Mn–O–O–Mn torsion angles different from zero) favors the release of triplet (ground state) O_2 [34, 44]. As shown in Fig. 4, this is the case for models **1** and **2**. The Mn–O–O–Mn torsion angles listed in Table 1 indicate symmetric peroxo coordination for both complexes **A** and **B**. The peroxo groups and the two Mn ions they bridge are approximately coplanar. Oxygen evolution has been observed from complex **A** but no information on its electronic ground state is available. It should be noted, however, that if complex **A** releases triplet oxygen this may not invalidate the above correlation; it could simply mean that a distortion of the peroxo bridge may occur just prior to the final oxidation step.

Dinuclear models

In order to compare oxygen activation energies at tetranuclear and dinuclear centers and to estimate the role of the Mn ions that do not participate directly in oxygen binding we have performed EH calculations on half of model **1**. This 'dimer', which retains the geometric features of its parent 'tetrameric' model **1**, is obtained by the 'cutting' process shown in Fig. 3. The oxygen–oxygen coupling energy barrier for this dimer was computed from the Walsh diagram obtained by distributing the electrons so as to simulate the reduction of $[Mn(IV)_2O(H_2O)_5(\mu\text{-}O)(\mu\text{-}HCOO)(O)_2]^{1-}$ to $[Mn(III)_2O(H_2O)_5(\mu\text{-}O)(\mu\text{-}HCOO)(\mu,\eta^2\text{-}O_2]^{1-}$. The

TABLE 2. Selected net charges and total energy variation ΔE (eV) for the proposed models. The values for the Mn ions directly bonded to dioxygen are underlined

Model[a]	Mn1	Mn2	Mn3	Mn4	$2O^{2-}/\mu,\eta^2\text{-}(O_2)^{2-}$	ΔE (eV)
$(\mathbf{1})^{5+}$	<u>1.79/1.70</u>	<u>1.72/1.51</u>	1.91/1.16	1.97/1.70	−1.55/−0.55	4.36
$(\mathbf{2})^{5+}$	1.95/1.23	<u>1.77/1.48</u>	<u>1.75/1.42</u>	1.96/1.39	−1.56/−0.56	4.16
$(\mathbf{3})^{4+}$	1.95/1.13	<u>1.68/1.54</u>	<u>1.75/1.42</u>	1.96/1.39	−1.56/−0.56	4.16
$(Dimer)^{1-}$	<u>1.74/1.09</u>	<u>1.79/0.67</u>			−1.55/−0.55	4.67

[a](**1**), (**2**): $Mn_4(H_2O)_{12}(\mu\text{-}O)(\mu\text{-}HCOO)_2(\mu_4,\eta^2\text{-}O_2H)(\mu,\eta^2\text{-}O_2)$; (**3**); $Mn_4Cl(H_2O)_{11}(\mu\text{-}O)(\mu\text{-}HCOO)_2(\mu_4,\eta^2\text{-}O_2H)(\mu,\eta^2\text{-}O_2)$; (dimer): $Mn_2O(H_2O)_5(\mu\text{-}O)(\mu\text{-}HCOO)(\mu,\eta^2\text{-}O_2)$.

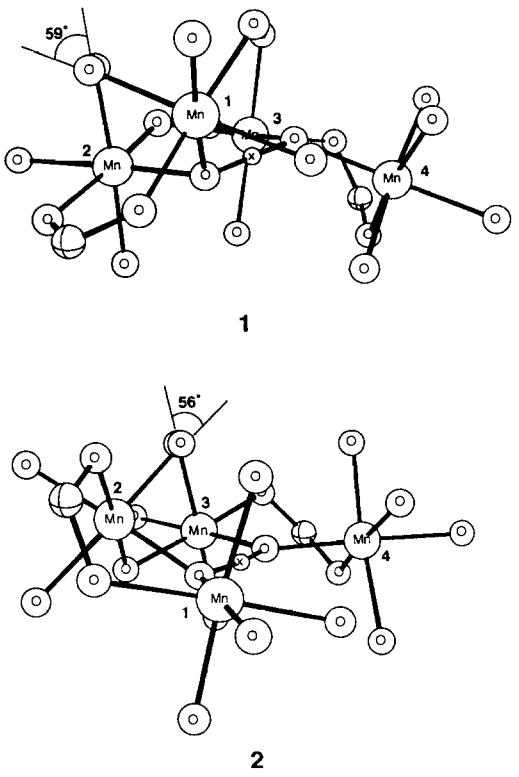

Fig. 4. View of models **1** and **2** along the O–O (peroxo) bond. The Mn–O–O–Mn torsion angles are marked.

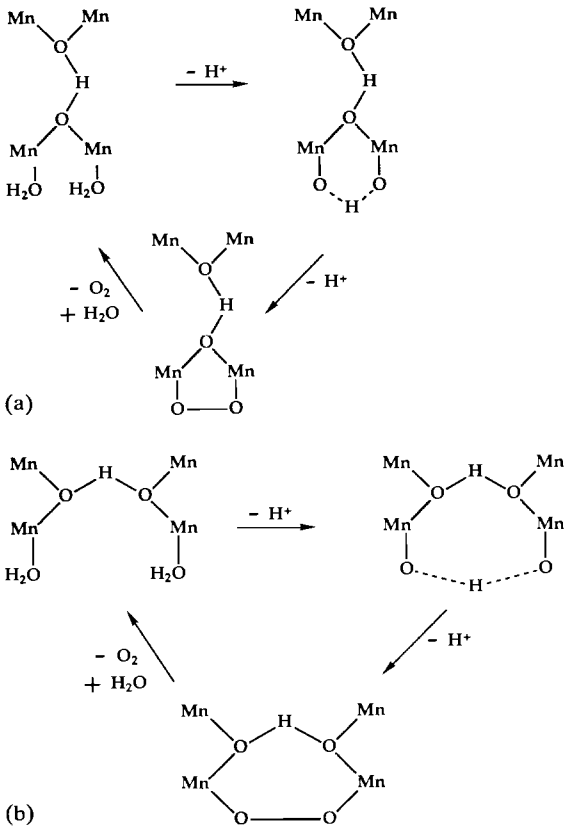

Fig. 5. Proposed mechanism for O_2 evolution: (a) topology based on model **1**, (b) topology based on model **2**.

results of Table 2 suggest that oxygen coupling for the dimeric complex is disfavored by approximately 0.3 eV with respect to the parent model **1**. Since the geometry of the 'dimer' has not been minimized, we suggest that the 0.3 eV difference is primarily an electronic effect due to the removal of two manganese ions. Thus, even if oxygen activation takes place at a dinuclear metal center, additionally aggregated metal ions might lower the energy barrier for oxygen coupling. We speculate that this effect might be one of the reasons why a polynuclear metal aggregate containing Mn and Ca is found at the active site of the WOC.

Proposal for oxygen evolution mechanism in the WOC of PSII

Based upon our calculations and in agreement with previous work we propose that in the WOC of PSII the O_2 evolution takes place at a dinuclear subset of the Mn_4 aggregate, namely at a Mn pair in which the Mn ions are separated by 2.7 Å (see Fig. 1).

A proposed mechanism for oxygen evolution is shown in Fig. 5. In this mechanism the water oxidation takes place in two, thermodynamically favorable, two-electron steps [45]. While we cannot entirely rule out that O_2 may result from the oxidation and coupling of the μ_4,η^2-(O–H–O) group, the mechanism suggested by our calculations is the formation of O_2 via the deprotonation of two terminal water molecules. A μ_2-peroxo S_4 state of the type present in models **1–3** is proposed as an intermediate. The notion that the μ_4,η^2-(O–H–O) group is not the source of O_2 is suggested by the observation that in PSII (at least) *two* protons are released from water only when the WOC reaches the S_3 or S_4 oxidation levels (Mn is mainly Mn(IV)). However, the μ_4,η^2-(O–H–O) unit, which contains only one proton, is stabilized by the Mn(III) and Mn(II) ions found in model **0**. While the O–H–O group *may* facilitate water deprotonation via H bonding it is more likely that the protonation level will decrease as the oxidation level of Mn increases. Thus, it is unlikely that *two* protons will be available for release in the μ_4,η^2-(O–H–O) units as the WOC reaches the S_3 or S_4 level. During the S_4 to S_0 transition when O_2 is released, however, protonation of metal–oxo bridges should favor the return of the WOC to the lower oxidation level. As mentioned above, only two Mn ions in models **1–3** are directly involved in peroxide binding. The remaining two Mn ions besides electronically favoring oxygen coupling, may also play an important structural role. The presence of multiple metal centers favors the formation of a higher number of hydrophilic, bridging oxo/hydroxo

groups which may be necessary for the proper functioning of the water oxidation catalysts, of such groups. The presence of hydrated calcium ions in the WOC may also favor the formation of oxo/hydroxo bridges.

In conclusion, we have introduced a computational methodology which combines a force field capable of optimizing geometries of inorganic materials with the extended Hückel method. Calculations of manganese models for the nascent S_4 state of the water oxidation catalyst of PSII using this methodology suggest that only two out of four Mn may be involved in oxygen–oxygen bond formation. A Mn-bound chloride ion is found not to lower the activation energy barrier. A new structural and mechanistic proposal, consistent with the current structural and functional understanding of WOC catalyzed oxidations is also presented. The favorable peroxo geometries we observe for our models combined with the low energy barrier for oxygen–oxygen coupling suggest that our models are good candidates for the S_4 state of the WOC of PSII.

Acknowledgement

Dr Suzanne E. Sherman is thanked for valuable suggestions and criticism during the preparation of the manuscript.

References

1 L.I. Simandi (ed.), *Catalytic Activation of Dioxygen by Metal Complexes,* Kluwer, Dordrecht, 1992.
2 R.S. Drago, *Coord. Chem. Rev., 117* (1992) 185.
3 D.T. Sawyer, *Oxygen Chemistry,* Oxford University Press, New York, 1991.
4 C.L. Hill (ed.), *Activation and Functionalization of Alkanes,* Wiley, New York, 1989.
5 A.E. Martell and D.T. Sawyer (eds.), *Oxygen Complexes and Oxygen Activation by Transition Metals*, Plenum, New York, 1988.
6 R.H. Holm, *Chem. Rev., 87* (1987) 1401.
7 R.A. Sheldon and J.K. Kochi, *Metal-Catalyzed Oxidations of Organic Compounds,* Academic Press, New York, 1981.
8 K. Weissermel and H.-J. Arpe, *Industrial Organic Chemistry*, Verlag Chemie, New York, 1978.
9 V.K. Yachandra, V.J. DeRose, M.J. Latimer, I. Mekerji, K. Sauer and M.P. Klein, *Science, 260* (1993) 675.
10 G.C. Dismukes, in J. Reedijk (ed.), *Bioinorganic Catalysis*, Marcel Dekker, New York, 1993, Ch. 10, p. 317.
11 R.J. Debus, *Biochim. Biophys. Acta, 1102* (1992) 269.
12 A.W. Rutherford, J.L. Zimmerman and A. Boussac, in J. Barber (ed.), *The Photosystems: Structure, Function and Molecular Biology,* Elsevier, Amsterdam, 1992, p. 179.
13 V.L. Pecoraro (ed.), *Manganese Redox Enzymes,* VCH, New York, 1992.
14 G.W. Brudvig, in A.J. Hoff (ed.), *Advanced EPR Applications in Biology and Biochemistry,* Elsevier, Amsterdam, 1990, p. 839.
15 J.E. Penner-Hahn, R.M. Fronko, V.L. Pecoraro, C.F. Yocum, S.D. Betts and N.R. Boweby, *J. Am. Chem. Soc., 112* (1990) 1549.
16 W.J. Coleman, *Photosynth. Res., 23* (1990) 1, and refs. therein.
17 G.N. George, R.C. Prince and S.P. Cramer, *Science, 243* (1989) 789.
18 G.T. Babcock, in J. Amesz (ed.), *New Comprehensive Biochemistry in Photosynthesis,* Vol. 15, Elsevier, Amsterdam, 1987, p. 125.
19 G.W. Brudvig, *J. Bioenerg. Biomemb., 19* (1987) 91.
20 G. Renger, *Angew. Chem., Int. Ed. Engl., 26* (1987) 643.
21 G.C. Dismukes, in U.L. Schramm and F.C. Welder (eds.), *Manganese in Metabolism and Enzyme Function,* Academic Press, London, 1986.
22 J. Amesz, *Biochim. Biophys. Acta, 726* (1983) 1.
23 B. Kok, B. Forbush and M. McGloin, *Photochem. Photobiol., 11* (1970) 457.
24 A.W. Rutherford, A. Boussac and J.-L. Zimmerman, *New J. Chem., 15* (1991) 491.
25 J. Mano, M.A. Takahashi and K. Asada, *Biochemistry, 26* (1987) 2495.
26 W.D. Frasch and R. Mei, *Biochim. Biophys. Acta, 891* (1987) 8.
27 L. Que, Jr. and A.E. True, *Prog. Inorg. Chem., 38* (1990) 98.
28 G.W. Brudvig and R.H. Crabtree, *Prog. Inorg. Chem., 37* (1989) 99.
29 R.T. Stibrany and S.M. Gorun, *Angew. Chem., Int. Ed. Engl., 29* (1990) 1156; a structurally related complex has been reported by W.H. Armstrong in ref. 13.
30 J.B. Vincent and G. Christou, *Adv. Inorg. Chem., 33* (1989) 197.
31 G. Christou, *Acc. Chem. Res., 22* (1989) 328.
32 K. Wieghardt, *Angew. Chem., Int. Ed. Engl., 28* (1989) 1153.
33 C.G. Young, *Coord. Chem. Rev., 96* (1989) 89.
34 D.M. Proserpio, R. Hoffmann and G.C. Dismukes, *J. Am. Chem. Soc., 114* (1992) 4374.
35 A.K. Rappé, C.J. Casewit, K.S. Colwell, W.A. Goddard III and W.M. Skiff, *J. Am. Chem. Soc., 114* (1992) 10024.
36 C.J. Casewit, K.S. Colwell and A.K. Rappé, *J. Am. Chem. Soc., 114* (1992) 10035.
37 C.J. Casewit, K.S. Colwell, A.K. Rappé, *J. Am. Chem. Soc., 114* (1992) 10046.
38 R. Hoffmann and W.N. Lipscomb, *J. Chem. Phys., 36* (1962) 2179, 3489.
39 R. Hoffmann, *J. Chem. Phys., 39* (1963) 1397.
40 J.H. Ammeter, H.-B. Burgi, J.C. Thibeault and R. Hoffmann, *J. Am. Chem. Soc., 100* (1987) 3686.
41 C. Mealli and D.M. Proserpio, *J. Chem. Educ., 66* (1990) 399.
42 U. Bossek, T. Weyhermülle, K. Wieghardt, B. Nuber and J. Weiss, *J. Am. Chem. Soc., 112* (1990) 6387.
43 R. Bhula, G.J. Gainsford and D.C. Weatherburn, *J. Am. Chem. Soc., 110* (1988) 7550.
44 Y. Nishida, *Inorg. Chim. Acta, 152* (1988) 73.
45 L.I. Krishtalik, *Bioelectrochem. Bioenerg., 23* (1990) 249.